The ICE_{XTD} of *Azoarcus* sp. CIB, an integrative and conjugative element with aerobic and anaerobic catabolic properties

María Teresa Zamarro, Zaira Martín-Moldes and Eduardo Díaz*

Environmental Biology Department, Centro de Investigaciones Biológicas, CSIC, Ramiro de Maeztu 9, 28040 Madrid, Spain.

*For correspondence. E-mail ediaz@cib.csic.es; Tel. +34918373112 ext. 4426; Fax +34915360432

Running title: The ICE_{XTD} element from *Azoarcus* sp. CIB

Originality-significance statement: Mobile genetic elements, such as integrative and conjugative elements (ICE), have been shown to play a major role in the aerobic degradation of environmental pollutants by many bacteria. However, ICEs have not yet been shown to be involved in anaerobic degradation of aromatic pollutants. In this work we report an ICE element from the β-proteobacterium *Azoarcus* sp. CIB that is able to expand the catabolic abilities of certain bacteria for the removal of aromatic hydrocarbons either in the presence or absence of oxygen. Our data suggest that ICEs also affects the biodegradation capacity of anaerobic bacteria to thrive in polluted environments.

Summary

Integrative and conjugative elements (ICE) play a major role in aerobic degradation of aromatic compounds, but they have not yet been shown to be involved in anaerobic degradation. We have characterized here the ICE$_{XTD}$ element which endows to the beta-proteobacterium *Azoarcus* sp. CIB with the ability to utilize aromatic hydrocarbons. The core region of ICE$_{XTD}$, which shows a remarkable synteny with that of ICE*clc*-like elements, allows its own intracellular and intercellular mobility. ICE$_{XTD}$ integrates at the tRNAGly of the host chromosome, but it can also excise to produce a ready to transfer circular form. The adaptation modules of ICE$_{XTD}$ represent a unique combination of gene clusters for aerobic (*tod* genes) and anaerobic (*bss-bbs* and *mbd* genes) degradation of certain aromatic hydrocarbons, e.g., toluene, *m*-xylene and cumene. Transfer of ICE$_{XTD}$ to other *Azoarcus* strains, e.g., *A. evansii*, confers them the ability to degrade aromatic hydrocarbons both aerobically and anaerobically. Interestingly, ICE$_{XTD}$ allows *Cupriavidus pinatubonensis*, a bacterium unable to degrade anaerobically aromatic compounds, to grow with *m*-xylene under anoxic conditions. Thus, ICE$_{XTD}$ constitutes the first mobile genetic element able to expand the catabolic abilities of certain bacteria for the removal of aromatic hydrocarbons either in the presence or absence of oxygen.

Introduction

Mobile genetic elements that carry genes for the degradation of pollutants, play a major role in the *in situ* spread and even *de novo* construction of catabolic pathways in bacteria (Springael and Top, 2004; Smillie *et al*., 2010; Wozniak and Waldor, 2010). Integrative and conjugative elements (ICEs) combine two properties, i.e., they are conjugative, which allows their horizontal spreading in the bacterial community, and they have the capacity to integrate into the bacterial host chromosome, which ensures their vertical transmission (Bellanger *et al.*, 2014). ICE elements are integrated at a specific site of the chromosome (*attB* site), usually a tRNA gene, and flanked by specific direct repeat sequences that define an attachment site on the right (*attR*) and left (*attL*) ends. Under certain conditions, ICE can excise from the chromosome, circularize as an extrachromosomal intermediate that is transferred to recipient cells via conjugation, and integrate into the host chromosome through site-specific recombination. ICEs have a conserved modular structure composed of three functional units (core region) carrying genes important for ICE function, i.e, the integration and excision, regulation and conjugation modules (Wozniak and Waldor, 2010; Bellanger *et al*., 2014). Interspersed among the conserved modules there are cargo genes that generally encode specific functions that allow for adaptation to the surrounding environment or other beneficial traits (Springael and Top, 2004; Juhas *et al*., 2009). Although new transposable elements are being uncovered, examples of ICEs carrying genes for the degradation of aromatic polluting compounds are still limited to date (Toleman and Walsh, 2011; Bellanger *et al*., 2014). The *clc* element (103 kb) from *Pseudomonas knackmussii* B13, that encodes degradation of chlorocatechols/aminophenols, has been thoroughly studied (Ravatn *et al*., 1998; Gaillard *et al*., 2006; Miyazaki *et al.*, 2011; Pradervand *et al*., 2014a, b; Miyazaki *et al*., 2015). ICE*clc*-like elements have been described in other bacteria that degrade aromatic compounds (Gaillard *et al*., 2006; Lechner *et al*., 2009). Other ICE elements carrying genes for degradation of aromatic compounds are those that belong to the Tn*4371*-like family (Nishi *et al.*, 2000; Toussaint *et al*., 2003; Van Houdt *et al.*, 2009; Ryan *et al.*, 2009; Ohtsubo *et al.*, 2012) or Tn*3*-like family (Yagi *et al.*, 2009; Jin *et al.*, 2011; Hickey *et al*., 2012). Interestingly, none of these ICEs characterized so far harbor genes for the anaerobic degradation of aromatic compounds.

The role of horizontal gene transfer in genome plasticity and evolution of aromatic degradation pathways has been proposed in some anaerobes such as in "*Aromatoleum aromaticum*" EbN1 strain (Rabus *et al*., 2005). However, the characterization of a mobile genetic element harboring genes for anaerobic degradation of aromatic compounds and its role in the adaptation to the presence of these carbon sources has not yet been reported. *Azoarcus* sp. CIB is a facultative anaerobic beta-proteobacterium capable of degrading either aerobically and/or anaerobically (using nitrate as terminal electron acceptor) a wide range of aromatic compounds including some toxic hydrocarbons such as toluene, *m*-xylene and cumene (López-Barragán *et al*., 2004; Carmona *et al*., 2009; Valderrama *et al.*, 2012; Juárez *et al*., 2013; Martín-Moldes *et al*., 2015). In addition to this free-living lifestyle, the CIB strain also shows an endophytic lifestyle (Fernández *et al*., 2014). Horizontal gene transfer and mobile genetic elements have been proposed to play a major role in the adaptation of *Azoarcus* sp. CIB to its different lifestyles. Thus, the ability of strain CIB to degrade aromatic hydrocarbons was suggested to be due to the presence of a putative integrative and conjugative element, ICE_{XTD}, in the genome of this bacterium (Martín-Moldes *et al*., 2015). In this work, we have characterized the ICE_{XTD} element and some of its cargo functions, e.g., pollutants degradation pathways, demonstrating that ICE_{XTD} becomes the first ICE described so far whose adaptation module allows the anaerobic degradation of aromatic hydrocarbons, and that combines this metabolic feature with the aerobic catabolism of this type of toxic compounds.

Results and discussion

Organization of the ICE_{XTD} element

A detailed analysis of the genome sequence of *Azoarcus* sp. CIB (Martín-Moldes *et al*., 2015) revealed a chromosomal element of 173,798 bp, named ICE_{XTD} (xylene and toluene degradation) element, that shows a significant similarity to the core region of ICE*clc*-like elements (Ravatn *et al*., 1998, Gaillard *et al*., 2006, Miyazaki *et al.*, 2011; Pradervand *et al*. 2014a,b; Miyazaki *et al.*, 2015). The ICE_{XTD} is located at the 3´end (*attB* site) of the AzCIB_R0069 gene for glycine-accepting tRNAs ($tRNAGly^{CCC}$) (Fig. 1A). Whereas the left end (*attL*) of ICE_{XTD} is formed by the last 23 bp of the tRNAGly (TTCGATTCCCATCGCCCGCTCCA) at chromosomal position 4,894,159, the right end (*attR*) of ICE_{XTD} is formed by a repetition of these 23 bp and is found at position

5,067,957. Supporting Information Table S1 shows the name, size, direction of transcription and predicted function for each of the 178 annotated ORFs. ICE_{XTD} is organized in at least four conserved gene modules, i.e., integration/excision, regulation, conjugation and partition, that constitute the core region, plus three non-conserved specific adaptation modules that contain cargo genes encoding mainly aromatic degradation pathways (Fig. 1A). Whereas the core region of ICE_{XTD} shows a GC content close to that of the genome (65.8% GC), the adaptation modules 1 (52% GC), 2 (73% GC) and 3 (59% GC), which are flanked by full or partial transposases (Fig. 1A, Supporting Information Table S1), show a significantly different GC content than the average GC content of the whole genome. These observations suggest that ICE_{XTD} was assembled primarily by different acquisition events of new cargo genes through horizontal gene transfer (Valderrama *et al*., 2012).

The integrase gene (int_{XTD}, AzCIB_4396), whose product should catalyze the site-specific integration and excision of the ICE_{XTD} element from the chromosome (Gaillard *et al.*, 2006), is located next to the *attL* sequence and oriented to the inward direction. In the vicinity of the int_{XTD} gene is located a regulatory module (AzCIB_4397-4399) that may be involved in the control of the expression of the integrase gene (Pradervand *et al*., 2014a,b) (Fig. 1A, Supporting Information Table S1). At the right end of ICE_{XTD} is located a partition/maintenance module (AzCIB_4569-4572), which also contains the AzCIB_4564 gene that encodes the InrR regulator likely involved in regulating the expression of the integrase gene (Minoia *et al*., 2008) (Fig. 1A, Supporting Information Table S1). The conjugation module of ICE_{XTD} is a large region syntenic to DNA conjugation modules of ICE*clc*-like elements (Gaillard *et al*., 2006; Guglielmini *et al.*, 2011; 2014; Bellanger *et al*., 2014; Miyazaki *et al*., 2015), but divided into two different regions, A and B (Fig. 1A, Supporting Information Table S1), by the insertion of the adaptation module 3 (see below).

A major physiological feature of *Azoacus* sp. CIB is its ability to degrade several aromatic hydrocarbons either aerobically (toluene, cumene) or anaerobically (toluene, *m*-xylene) (López-Barragán *et al*., 2004; Blázquez *et al*., 2008; Juárez *et al*., 2013; Martín-Moldes *et al.*, 2015). Interestingly, the cargo genes present in ICE_{XTD} are predicted to be mainly devoted to the catabolism (adaptation modules 1 and 3) and efflux (adaptation module 2) of these aromatic hydrocarbons (Fig. 1A), thus suggesting that ICE_{XTD} is an evolutionary acquisition of *Azoarcus* sp. CIB for the degradation of

such compounds. The adaptation module 1 harbors a *tod* cluster that contains genes orthologous to those described for the aerobic degradation of aromatic hydrocarbons, e.g., toluene, to TCA cycle intermediates via an initial dioxygenation step followed by a *meta*-cleavage pathway (Fig. 1B, Supporting Information Table S1) (Eaton and Timmis, 1986; Zylstra and Gibson, 1989; Pflugmacher *et al.*, 1996; Choi *et al.*, 2003). The genetic organization of the *tod* genes suggests that they constitute a single operon (Supporting Information Table S1). As expected, the *tod* genes appear to be specifically induced when *Azoarcus* sp. CIB grows aerobically with toluene relative to their expression in benzoate (control condition) (Fig. 2A). Studies on the substrate specificity of the *tod* pathway revealed that the TodF hydrolase behaves as a limiting step in terms of channeling different substrates into TCA cycle intermediates because of its narrow substrate preference (Furukawa *et al.*, 1993; Seah *et al.*, 1998). However, it is worth noting that the *tod* cluster of ICE_{XTD} is endowed with two different *todF* genes, i.e, *todF1* (AzCIB_4408) which shows similarity to genes encoding 2-hydroxy-6-oxo-6-methylhexa-2,4-dienoate hydrolases involved in toluene degradation (Choi *et al.*, 2003), and *todF2* (AzCIB_4406) which shows similarity to genes encoding 2-hydroxy-6-oxo-7-methylocta-2,4-dienoate hydrolases involved in cumene degradation (Fig. 1B; Supporting Information Table S1) (Eaton and Timmis, 1986; Pflugmacher *et al.*, 1996), which may represent a new strategy to broaden the substrate range of the tod degradation pathway in certain bacteria.

The adaptation module 2 encodes some proteins of unknown function and two putative efflux systems, i.e., an ABC-2 type exporter (AzCIB_4432-4434) and a RND-type efflux system (AzCIB_4435-4438) (Supporting Information Table S1), that are significantly induced when *Azoarcus* sp. CIB becomes exposed to a sudden toluene shock (Fig. 2C). Thus, these transport systems might be involved in the efflux of toxic compounds (Ramos *et al.*, 2015) as an adaptation mechanism of *Azoarcus* sp. CIB to the presence of aromatic hydrocarbons.

The adaptation module 3 harbors the AzCIB_4501-4526 cluster that contains the *bss-bbs* genes orthologous of those encoding the peripheral pathway for the anaerobic degradation of toluene/*m*-xylene in different bacteria (Fig. 1B, Supporting Information Table S1) (Carmona *et al.*, 2009; Boll *et al.*, 2013; Wöhlbrand *et al.*, 2013; Kim *et al.*, 2014; Bozinovski *et al.*, 2014). Hence, adaptation module 3 should confer to *Azoarcus* sp. CIB the ability for the anaerobic conversion of toluene and *m*-xylene to benzoyl-

CoA and 3-methylbenzoyl-CoA, respectively. Benzoyl-CoA is further dearomatized and degraded by the benzoyl-CoA central pathway constituted by the Bzd proteins which are encoded by the *bzd* genes located outside the ICE_{XTD} element (Fig. 1B) (López-Barragán *et al*., 2004; Carmona *et al*., 2009, Martín-Moldes *et al*., 2015). On the contrary, 3-methylbenzoyl-CoA is degraded by the 3-methylbenzoyl-CoA pathway constituted by the Mbd enzymes encoded by the *mbd* genes (AzCIB_4474-4500) (Juárez *et al*., 2013; 2015) which are located adjacent to the *bss-bbs* genes within adaptation module 3 (Fig. 1B, Supporting Information Table S1). Accordingly, *Azoarcus* sp. CIB was shown to induce the *bss-bbs* genes when grown anaerobically on either toluene or *m*-xylene (Fig. 2B), and the *mbd* genes reached the highest induction when the cells grew anaerobically on *m*-xylene (Fig. 2B).

In vivo *tracking of* ICE_{XTD} *in* Azoarcus *sp. CIB*

ICE elements can be present in the host cell both integrated into the chromosome or excised as multiple circular copies behaving as replicating ICEs (Juhas *et al*., 2009; Bellanger *et al*., 2014). We have tracked the location of ICE_{XTD} in *Azoarcus* sp. CIB cells by a PCR amplification strategy with selected oligonucleotide pairs. By using the right combination of primers we could distinguish between, i) chromosomal insertion, ii) chromosomal excision, and iii) extrachromosomal circular form of ICE_{XTD} (Fig. 3A). PCR amplifications yielded bands that are consistent with the three possible locations, thus confirming that the *Azoarcus* sp. CIB population contains cells where the ICE_{XTD} is integrated into the chromosome as well as cells where ICE_{XTD} did excise from the chromosome to produce a circular form and the host genome was repaired upon excision (Fig. 3B). The nucleotide sequences of the different amplified products perfectly matched the expected sequences. Thus, the circular form of ICE_{XTD} was formed by the recombination between the TTCGATTCCCATCGCCCGCTCCA sequences located at the extreme ends of this element.

To visualize the extrachromosomal circular form of the ICE_{XTD} element and confirm its molecular size, we used pulsed-field gel electrophoresis of *Azoarcus* sp. CIB cells embedded in agarose plugs. Cells were digested with S1 nuclease to linearize covalently closed circular DNA (Barton *et al*., 1995), and Southern blot with a specific DNA probe of ICE_{XTD}, e.g., the *bssA* gene located within the adaptation module 3. As shown in Figure 3C, a band corresponding to the extrachromosomal form of ICE_{XTD}

element was observed, and it had a size that corresponds to that of a monomer of the covalently closed circular ICE$_{XTD}$ element. Taken together, these data suggest that ICE$_{XTD}$ can be excised from the chromosome of a certain population of *Azoarcus* sp. CIB, and eventually remains in such host cells as a monomeric circular intermediate.

Significant differences were not observed in the intensities of the different PCR-amplified bands when culturing *Azoarcus* sp. CIB in the presence of different carbon sources (e.g., succinate, benzoate, toluene, *m*-xylene) or terminal electron acceptors (oxygen, nitrate) (data not shown). However, we observed that the amplicons of the circular and repaired chromosome forms from exponential phase anaerobic cultures showed a substantially weaker signal compared to those obtained with stationary phase cultures (Fig. 3B), suggesting that the subpopulation of CIB cells that harbor an extrachromosomal ready to transfer ICE$_{XTD}$ element increases upon entry into stationary growth phase. This behavior resembles that previously described in ICE*clc*, which is mainly excised from the chromosome and transfer competent when the host cells reach stationary phase (Miyazaki *et al*., 2012).

Isolation and characterization of the Azoarcus *sp. CIBT strain*

We have isolated by serendipity after long term routinely anaerobic growth with benzoate a spontaneous *Azoarcus* sp. CIB mutant strain, named *Azoarcus* sp. CIBT strain (Table 1), that was unable to grow anaerobically with toluene. We then observed that strain CIBT was also unable to grow with *m*-xylene under anoxic conditions, and with toluene/cumene in the presence of oxygen (Table 2), suggesting that it could have arisen from parental strain CIB by the spontaneous loss of an extrachromosomal ICE$_{XTD}$ element. To confirm this assumption, we checked whether ICE$_{XTD}$ was present in *Azoarcus* sp. CIBT cells by PCR amplification with selected oligonucleotide pairs as we did before with the wild-type strain CIB. Whereas no amplicons corresponding to the integrated form and/or the extrachromosomal circular form of ICE$_{XTD}$ were observed, a band from the bacterial repaired chromosome was clearly visible (Fig. 3B), and the sequencing of this chromosomal region confirmed the lack of ICE$_{XTD}$ in *Azoarcus* sp. CIBT. As expected, pulsed-field gel electrophoresis of *Azoarcus* sp. CIBT cells embedded in agarose plugs revealed the absence of the extrachromosomal form of ICE$_{XTD}$ in these cells (Fig. 3C). All these results taken together indicate that *Azoarcus* sp. CIBT is a derivative of the wild-type CIB strain lacking the complete ICE$_{XTD}$

element, and they confirm the physiological role of this ICE element as an adaptive acquisition that expands the metabolic versatility of strain CIB towards aromatic hydrocarbons.

ICE$_{XTD}$ is a conjugative self-transferable element

Despite ICE*clc*-like elements are widely distributed in gamma- and beta-proteobacteria, only a few have been demonstrated so far to transfer to other cells (Roche *et al*., 2010; Smillie *et al*., 2010). The presence of extrachromosomal circular copies of ICE$_{XTD}$ in the *Azoarcus* sp. CIB population (Fig. 3), and the existence of a conjugation module in the modular architecture of ICE$_{XTD}$ (Fig. 1A), suggest that this element can be self-transferable by conjugation. To demonstrate the autonomous intercellular transfer of ICE$_{XTD}$, we performed mating experiments with two *Azoarcus* sp. CIB-derived strains. *Azoarcus* sp. CIBTRif (Table 1) is a rifampicin-resistant derivative of strain CIBT that was used as recipient in the conjugation experiments. *Azoarcus* sp. CIBd*tolR* strain was used as donor because it carried a kanamycin resistant gene inserted into the ICE$_{XTD}$ (ICE$_{XTD}$-Km) which did not prevent growth of the host cells with aromatic hydrocarbons (Table 1). The donor strain was mated with the recipient strain and transconjugants were selected by their resistance to rifampicin and kanamycin. It was observed the appearance of transconjugants, *Azoarcus* sp. CIBTRifICE$_{XTD}$, in the medium containing the appropriate combination of antibiotics with transfer frequencies of about 2 x 10^{-7} transconjugants per donor cell on average. A PCR-based analysis to confirm the presence of ICE$_{XTD}$-Km in the genome of the *Azoarcus* sp. CIBTRifICE$_{XTD}$ transconjugants was then conducted. As with the wild-type CIB strain (Fig. 3B), three different amplicons corresponding to the integrated, excised and extrachromosomal forms of ICE$_{XTD}$-Km were observed (Supporting Information Fig. S1). Moreover, the integration at the *attB* site of tRNAGly^{CCC} was confirmed by sequencing the amplicon derived from the integrated form of ICE$_{XTD}$-Km. Interestingly, the *Azoarcus* sp. CIBTRifICE$_{XTD}$ transconjugants recovered the ability to grow aerobically in the presence of toluene/cumene, and they were also able to grow anaerobically with toluene/*m*-xylene (Table 2). All these data reveal that the core region of ICE$_{XTD}$ is fully functional allowing its own intracellular (integrase gene) or intercellular (conjugation genes) mobility, and that ICE$_{XTD}$ behaves as a conjugative mobile genetic element capable to confer the ability to use aromatic hydrocarbons to *Azoarcus* sp. CIB cells.

ICE$_{XTD}$ *effects on host fitness*

ICE$_{XTD}$ becomes a fitness element when *Azoarcus* sp. CIB grows with aromatic hydrocarbons because they are uncommon growth substrates or even toxic to most bacteria (Ramos *et al.*, 2015; Rabus *et al.*, 2016). On the contrary, it could be anticipated that ICE$_{XTD}$ might have a fitness cost when the CIB strain grows with other carbon sources, e.g., benzoate, that do not require the presence of ICE$_{XTD}$. We have checked the influence of ICE$_{XTD}$ on host fitness by growing *Azoarcus* sp. CIB cells anaerobically with benzoate, and by tracking the presence of ICE$_{XTD}$ through PCR-analyses and testing growth with toluene. Growth experiments carried out for 80 generations in subsequent batch transfers did not show a significant loss of the ICE$_{XTD}$ element in the *Azoarcus* sp. CIB population (data not shown). Then, competition assays were performed during batch growth to examine whether the fitness of *Azoarcus* sp. CIBTRifICE$_{XTD}$ was reduced by the presence of the ICE$_{XTD}$ element compared to that of strain *Azoarcus* sp. CIBTRif that lacks such ICE element. Firstly, no significant differences in batch growth rates were observed between both strains when they were independently cultivated with benzoate either aerobically or anaerobically (Fig. 4A). Moreover, neither of the two populations significantly outcompeted the other in batch mixtures grown for 60 generations in subsequent batch transfers (Fig. 4B). Thus, one may conclude that the ICE$_{XTD}$ element imposes very little fitness loss on *Azoarcus* sp. CIB under general growth conditions that are not selective for the presence of this mobile element, just as no fitness loss was imposed on *Pseudomonas aeruginosa* PAO1 by the presence of the ICE*clc* element (Gaillard *et al.*, 2008). The relatively small fitness impairment may be one of the reasons why ICE*clc*-like elements have established themselves in a large diversity of bacterial genomes and play such an important role in bacterial evolution (Gaillard *et al.*, 2008; Miyazaki *et al.*, 2015).

Conjugal transfer of ICE$_{XTD}$ *to heterologous hosts: expanding the metabolic capabilities of bacteria to degrade aromatic hydrocarbons*

The host range of ICEs has been poorly studied so far and it can be very different from one element to another (Bellanger *et al.*, 2014). We have demonstrated above that ICE$_{XTD}$ could be successfully transferred from *Azoarcus* sp. CIB to *Azoarcus* sp. CIBT strain. To check whether ICE$_{XTD}$ could be also transferred to other *Azoarcus* species, we performed mating experiments between *Azoarcus* sp. CIBd*tolR* (ICE$_{XTD}$-Km) as donor

strain and *Azoarcus evansii*, a well-studied prototype strain within the *Azoarcus* genus (Anders *et al*., 1995; Fuchs *et al*., 2011), as recipient. We obtained kanamycin resistant transconjugants with an efficiency of 1.7 x 10^{-8} per donor cell. A PCR-based analysis confirmed the presence of the integrated, excised and some extrachromosomal forms of ICE_{XTD}-Km in *A. evansii*RifICE_{XTD} transconjugants (Supporting Information Fig. S1). Although *A. evansii* is able to degrade several aromatic acids in the presence or absence of oxygen, it cannot use aromatic hydrocarbons (Anders *et al*., 1995; Fuchs *et al*., 2011). Interestingly, the *A. evansii*RifICE_{XTD} transconjugants were able to grow with toluene and cumene as sole carbon sources under oxic conditions, and they grew also with toluene and *m*-xylene under anoxic conditions (Table 2). These results indicate that ICE_{XTD} is a conjugative element that can be transferred among *Azoarcus* species, where it confers the ability to degrade aromatic hydrocarbons, e.g. toluene, *m*-xylene and cumene, both aerobically and anaerobically.

To study further whether ICE_{XTD} could be transferred to other bacteria outside the *Azoarcus* genus, we have used as recipient strain the beta-proteobacterium *Cupriavidus pinatubonensis* JMP289 (Don and Pemberton, 1981). We could obtain kanamycin resistant transconjugants of *C. pinatubonensis* with an average efficiency of 4.8 x 10^{-7} per donor cell. The *C. pinatubonensis* JMP289ICE_{XTD} transconjugants were checked by PCR-based analysis, and the presence of the integrated, excised and extrachromosomal forms of ICE_{XTD}-Km was confirmed (Supporting Information Fig. S1). The acquisition of ICE_{XTD} by *C. pinatubonensis* did not lead to a fitness loss as revealed by the absence of any detrimental effect on the exponential phase of a bacterial culture of *C. pinatubonensis* JMP289ICE_{XTD} grown with succinate (Fig. 5A). It is worth noting that when *C. pinatubonensis* JMP289ICE_{XTD} was used as donor strain and *Azoarcus* sp. CIBT as recipient in mating experiments, we could observe retrotransfer of the ICE_{XTD}-Km element back to the *Azoarcus* cells with a frequency of 9 x 10^{-8} transconjugants per donor cell. These data confirm that ICE_{XTD} encodes all necessary functions for self-transfer from heterologous hosts, and that conjugative transfer and mobilization of ICE_{XTD} may occur with a similar frequency in the two gene flow directions.

The functionality of ICE_{XTD} in *C. pinatubonensis* was tested by checking the expression of some of its cargo genes. Although *C. pinatubonensis* is able to degrade more than 60 different aromatic compounds under oxic conditions, it is unable to use

cumene as sole carbon and energy source (Pérez-Pantoja *et al*., 2008). As in the case of *A. evansii*, *C. pinatubonensis* JMP289ICE$_{XTD}$ transconjugants were able to use cumene as sole carbon source under oxic conditions. More interestingly, in contrast to the parental *C. pinatubonensis* JMP289 strain that is unable to use aromatic compounds under anoxic conditions, the *C. pinatubonensis* JMP289ICE$_{XTD}$ transconjugants grew anaerobically (using nitrate as electron acceptor) on *m*-xylene as sole carbon source (Fig. 5B, Table 2). To our knowledge, these results constitute the first example of successful horizontal transfer of gene clusters involved in the anaerobic catabolism of aromatic hydrocarbons to bacteria that are unable to degrade these compounds in the absence of oxygen.

All these data taken together reveal that the cargo genes of ICE$_{XTD}$ are functional in heterologous hosts, and they suggest the use of ICE$_{XTD}$ as a new biotechnological tool to expand the catabolic abilities of some biocatalysts for the removal of toxic aromatic hydrocarbons either in the presence or absence of oxygen.

Evolutionary considerations and conclusions

A genome search among all *Azoarcus* strains and closely related bacteria of the *Rhodocyclaceae* family so far sequenced revealed that two strains, *A. toluclasticus* MF63 (Accession no. NZ_ ARJX00000000.1) and "*Aromatoleum aromaticum*" EbN1 (Rabus *et al*., 2005), contain ICE$_{XTD}$-like elements. Comparative analyses suggest that the evolution of ICE$_{XTD}$ and its close relatives primarily took place by acquisition of different cargo genes into the adaptation modules. Whereas ICE^{MF63} (110 kb) harbors an adaptation module with gene clusters predicted to encode heavy metals resistance, the ICE^{EbN1} (110 kb) harbors an adaptation module that contains the *ebd-apc* gene cluster for the anaerobic degradation of ethylbenzene (Rabus *et al*., 2002) (Fig. 6). Interestingly, although the MF63 and EbN1 strains are able to degrade toluene anaerobically, their *bss-bbs* genes are not located within their ICE elements, in contrast to the situation observed in the CIB strain. As in the case of ICE$_{XTD}$, ICE^{MF63} and ICE^{EbN1} are integrated at the tRNAGly located downstream of a *thi* gene, and all of them have identical *attL/attR* sites in their respective chromosomes (Fig. 6). Downstream of the *attR* site of the ICE^{EbN1} element, a second copy of a truncated integrase, a relaxase and several paralogs of T4SS proteins can be identified (Fig. 6), suggesting the evidence of previous accretion and subsequent deletions processes (Bellanger *et al*., 2014). Other

Azoarcus strains that do not harbor an ICE$_{XTD}$-like element, e.g., *Azoarcus* sp. KH32C (Nishizawa *et al*., 2012), show the same *thiS*-tRNAGly-*sodC* chromosomal gene arrangement observed in *Azoarcus* sp. CIB, which provides further support to the assumption that ICE$_{XTD}$-like elements have been recruited by some *Azoarcus* strains through site-specific insertion at a conserved chromosomal region for their adaptation to use or tolerate pollutants.

In summary, we have characterized for the first time an ICE element present in beta-proteobacteria of the *Rhodocyclaceae* family (Martín-Moldes *et al*., 2015). The adaptation modules 1-3 of ICE$_{XTD}$ constitute the largest (104 kb) cargo region described so far for ICE*clc*-like elements, and they represent a unique combination of gene clusters for aerobic (*tod* genes, adaptation module 1) and anaerobic (*bss-bbs* and *mbd* genes, adaptation module 3) degradation of certain aromatic hydrocarbons, e.g., toluene, *m*-xylene and cumene, as well as clusters encoding putative hydrocarbon efflux pumps (adaptation module 2). ICE$_{XTD}$ constitutes, to the best of our knowledge, the first mobile genetic element reported that is able to expand the catabolic abilities of certain bacteria for the removal of toxic aromatic hydrocarbons either in the presence or absence of oxygen. Moreover, our work extends the current knowledge on the adaptive traits of ICEs in bacteria, and suggests that ICEs become key elements shaping also the biodegradative capacity of anaerobic bacteria to thrive in polluted environments.

Experimental Procedures

Bacterial strains and growth conditions

The bacterial strains used in this work are listed in Table 1, and they were grown at 30ºC. *Azoarcus* strains were grown anaerobically in MC medium using 10 mM nitrate as terminal electron acceptor as described previously (López-Barragán *et al*., 2004) and the appropriate carbon source, i.e., 0.2% pyruvate, or 3 mM benzoate. Aromatic hydrocarbons (toluene, *m*-xylene) were added at 250 mM in 2,2,4,4,6,8,8-heptamethylnonan as an inert carrier phase. *Azoarcus* strains were also grown aerobically in MC medium without nitrate. *Cupriavidus pinatubonensis* JMP 289 cells were grown aerobically in Lysogeny Broth (LB) mediun (Sambrook and Rusell, 2001), or MC medium without nitrate and with 0.2% succinate, or anaerobically in minimal MC medium with 10 mM nitrate and 125 mM *m*-xylene in 2,2,4,4,6,8,8-heptamethylnonan as an inert carrier phase. Under oxic conditions, aromatic

hydrocarbons (toluene, cumene) were added directly to the MC medium at 1 mM. Where appropriate, antibiotics were added at the following concentrations: gentamycin, 7.5 μg ml^{-1}; kanamycin, 50 μg ml^{-1}; rifampicin, 50 μg ml^{-1}. Bacterial growth was monitored by measuring the absorbance at 600 nm (A_{600}). The spontaneous rifampicin-resistant mutants used in this work were isolated by plating cultures at the stationary growth phase on solid medium containing rifampicin. 16S-rDNA PCR analyses were performed to confirm the identity of rifampicin-resistant mutants.

Molecular biology techniques

Standard molecular biology techniques were performed as previously described (Sambrook and Russel, 2001). PCR was used to detect the integrated, excised and extrachromosomal forms of ICE_{XTD}. Oligonucleotides P1-P4 are listed in Supporting Information Table S2, and their targeted genomic locations are illustrated in Figure 3A. PCR reactions were performed in a final volume of 50 μl containing 1 unit of AmpliTaq DNA polymerase (Biotools), 500 μM of each dNTP, 0.04% DMSO and 0.4 μM of each primer pair. PCR amplification conditions were as follows: (i) 1 initial cycle of 5 min at 95ºC, 1 min at 60ºC and 2 min at 72ºC; (ii) 30 cycles of amplification of 1 min at 95ºC, 1 min at 60ºC and 1 min at 72ºC. PCR products were purified with Gene-Clean Turbo (Q-BIOgene) and sequenced with fluorescently labelled dideoxynucleotide terminators (Sanger *et al.*, 1977) and AmpliTaq FS DNA polymerase (Applied Biosystems) in an ABI Prism 377 automated DNA sequencer (Applied Biosystems).

Conjugational transfer assays of the ICE_{XTD} element

To check the transfer of ICE_{XTD} we performed bacterial conjugation in filter mating experiments (de Lorenzo and Timmis, 1994). Donor and recipient cells were grown until the end of the exponential growth phase. *Azoarcus* sp. CIB containing the ICE_{XTD}-Km element was used as donor, and it was grown anaerobically in MC medium containing kanamycin and pyruvate as carbon source. Recipient cells were aerobically grown in MC medium with an appropriate carbon source or, in case of *C. pinatubonensis* JMP289, in LB medium, containing rifampicin. All cells were centrifuged and washed with sterile salt solution to remove antibiotics, and then resuspended in 50 μl of sterile salt solution. Donor and recipient cells were mixed 1:1

and spotted on sterile nitrocellulose filters (0.45 μm, Millipore) placed on MC agar plus succinate plates and incubated 12 h at 30ºC. After incubation, the cells of the filter were suspended in fresh medium and plated aerobically on selective kanamycin- and rifampicin-containing MC medium with the appropriate carbon source to counterselect the donor cells, i.e., i) 10 mM glutarate when using as recipient *Azoarcus* sp. CIBTRif cells; ii) 3 mM 4-hydroxybenzoate when using as recipient *C. pinatubonenesis* JMP289 cells; and iii) 3 mM 2-aminobenzoate when using as recipient *A. evansii*Rif cells. Conjugative transfer frequencies were calculated as the number of transconjugant cells per number of donor bacterial cells present in each mating. To confirm the identity of the transconjugant cells, PCR reactions were performed with genomic DNA by using primers that amplify the 16S ribosomal DNA (Supporting Information Table S2), and the PCR products were analyzed by sequencing. The presence of the ICE_{XTD} element in the transconjugants was also confirmed by PCR analyses (see above).

To check retrotransfer of ICE_{XTD}-Km from *C. pinatubonensis* JMP289ICE_{XTD}, used as donor strain, to a gentamycin resistant *Azoarcus* sp. CIBT strain containing the pIZ1016 vector (Moreno-Ruiz *et al.*, 2003), exconjugants were selected on kanamycin- and gentamycin-containing MC medium using 10 mM glutarate as carbon source.

Tracking the extrachromosomal form of ICE_{XTD} by pulse field gel electrophoresis and nuclease S1 treatment

Azoarcus sp. CIB and *Azoarcus* sp. CIBT were grown anaerobically in MC medium with pyruvate to reach an A_{600} of 0.6. Cells from 80 ml culture were collected by centrifugation at 4.500 × *g* for 10 min, washed with cold 10 mM Tris pH 8.0, 1 M NaCl buffer, resuspended in the same solution to reach an A_{600} of 4.0, and keep on ice for 15 min. Equal volumes of cell suspension and molten 1% (wt/vol) low-melting-temperature agarose (Bio-Rad) were mixed and dispensed into molds on ice. Once solidified, the gel blocks were incubated in 3 ml lysis buffer (6 mM Tris HCl pH 8.0, 1 M NaCl, 100 mM EDTA, 0.2% sodium deoxycholate, 0.5% Brij-58, 0.5% Sarkosyl) with 20 μg/ml RNase A (Roche) and 1mg/ml lysozyme (Sigma) at 37°C for 1 h. The lysis buffer was then replaced by Proteinase K solution (0.5 M EDTA pH 9.0, 1% (wt/vol) Sarkosyl, 1 mg/ml proteinase K (Roche)), and the gel blocks were incubated at 50°C overnight. Gels blocks were then incubated twice in TE buffer (10 mM Tris HCl pH 8.0, 1 mM EDTA) with 40 μg/ml PMSF for 1 h at 50°C. For long-term storage,

blocks were kept at 4°C in 0.5 M EDTA (pH 9.0). For S1 nuclease digestion of single slices, they were first washed twice for 30 min in TE buffer and equilibrated in 2 ml of the appropriate buffer for 30 min. Then, each agarose plug was incubated for 1 h at 37°C with 1 µl (100 U) of S1 nuclease of *Aspergillus oryzae* (Sigma) in 1 ml of 50 mM NaCl, 30 mM sodium acetate pH 4.5, 5 mM $ZnSO_4$. The reaction was stopped by transferring the slices to TE buffer on ice (Barton *et al.*, 1995). Slices were applied to the wells of a 14.5 x 13 cm, 1.5% (w/v) agarose gel, prepared in 0.5x TBE buffer (45 mM Tris HCl pH 8, 45 mM boric acid, 1 mM EDTA) and run at 14ºC in a clamped homogeneous electric field (CHEF) electrophoresis using a CHEF-DR II system (Bio-Rad) at 200 V in 0.5x TBE for 20 h with pulse time increasingly from 0.1 to 10 s. Concatemers of Lambda DNA (New England Biolabs) were used as size markers. After electrophoresis, the gels were stained with GelRed (Biotium).

Probe preparation and southern hybridization

The probe DNA used for detection ICE_{XTD} was a 576-bp *bss*A gene fragment obtained by PCR-amplification from *Azoarcus* sp. CIB genomic DNA with oligonucleotides BssA new 5' and BssA new 3´ (Supporting Information Table S2). The bssA probe was labelled with [α^{32}P]dATP (6000 Ci/mmol; 20 mCi/ml; Perkin-Elmer) by adding a random hexanucleotide mixture and 1 µl Klenow fragment of *E. coli* DNA polymerase (5 U/µl; Promega) for 90 min at 37ºC. The reaction was stopped with 2 µl of 0.5 M EDTA solution. To remove the unincorporated nucleotide, the total reaction volume was filtered through a VIVASPIN 500 column (Sartorius Stedim Biotech GmbH) according to the manufacturer instructions.

Pulse field gels were pressure blotted onto a NYTRAN N membrane (Whatman). To this end, the stained gel was irradiated by UV light for 2 min, denatured with a solution of 1.5 M NaCl, 0.5 M NaOH for 30 min, and finally neutralized in a solution of 1.5 M NaCl, 0.5 M Tris HCl pH 7.2, 1 mM EDTA for 30 min. The DNA was transferred in 20x SSC (1x SCC is 150 mM NaCl, 15 mM trisodium citrate pH 7, 0.05 mM EDTA) to the nylon membrane overnight at room temperature. The membrane was removed from the gel and washed with water for 30 s, then the DNA was fixed on the membrane with UV light for 5 min each face. Prehybridizations were performed with 20 ml of hybridization buffer (6x SCC, 1% SDS with powdered milk 1 gram per 50 ml and 200 µg denatured herring sperm DNA of a solution at 1 mg/ml), at 65ºC for

approximately 5 h. Then the hybridization was carried out by adding the ^{32}P-bssA DNA probe to the hybridization buffer at 65ºC overnight, followed by washing with a solution of 2x SCC, 0.1% SDS for 10 min at 65ºC and once with a solution of 1x SCC, 0.1% SDS for 10 min at 65ºC. Autoradiographs were produced by exposing Amersham Hyperfilm MP (GE Healthcare) for 24-48 h at -80ºC using intensifying screen.

Toluene shocks assays

Azoarcus sp. CIB strain was grown anaerobically in MC medium containing 0.2% pyruvate. When cultures reached mid-exponential phase, they were divided into two halves: 20 mM toluene (saturation concentration) was added to one half and the other was used as control. Cultures were then incubated with shaking for 2 additional hours, and total RNA was isolated.

RNA extraction and RT-PCR amplification

Total RNA was extracted from early-exponential phase bacterial cultures using High Pure Isolation kit (Roche), and then DNase I-treated according to the manufacturer´s instructions (Ambion). The concentration and purity of the RNA samples were assessed using a Nanophotometer Pearl (IMPLEN) according to the manufacturer's protocols. Synthesis of total cDNA was performed by using the Transcriptor First Strand cDNA Synthesis kit (Roche) in 20-µl reactions containing 1 µg of RNA, 1 mM of each dNTP, 10 units of reverse transcriptase, 20 units of Protector RNase Inhibitor, and 60 µM random hexamers, provided by the manufacturer. The RNA and hexamers were initially heated at 65 °C for 10 min and following the addition of the rest of the components, samples were incubated at 25°C for 10 min and then at 55°C for 30 min. Reactions were terminated by incubation at 85°C for 5 min. RT-PCR amplifications were carried out with one denaturation cycle (95 °C for 5 min), followed by 25 cycles of amplification (95 °C for 1 min, 60 °C for 1 min, and 72 °C for 40 s). Oligonucleotides TodC1 5' and TodC1 3', BssA new 5' and BssA new 3', BbsD 524.5' and BbsD new 3', MbdO F3 and MbdO R3, AcrB 5' and AcrB 3' and ABC-2 5' and ABC-2 3' (Table S2) were used to amplify transcripts from genes *todC1, bssA, bbsD, mbdO,* AzCIB_4437 and AzCIB_4432, respectively. Oligonucleotides HK 5' and HK 3' (Supporting Information Table S2) were used to amplify transcripts from the *dnaE* gene (α-subunit DNA polymerase) used as an internal control. The expression of the internal control was shown to be similar across all samples analysed. The PCR-amplification products were

visualized in agarose gels stained with Gel Red in a Chemi Doc Touch Images Equipment. The intensity of the bands was quantified using the Image Lab 5.2.1 software (BioRad).

Acknowledgments

We thank J.L. García for helpful discussions, A. Valencia for technical assistance and Secugen S.L. for DNA sequencing. This work was supported by grants BIO2012-39501 and PCIN-2014-113; European Union FP7 Grant 311815; Fundación Ramón-Areces XVII CN. Z.M.-M. was the recipient of Research Personnel Formation (FPI) fellowship from the Ministry of Economy and Competitiveness of Spain.

References

Anders, H.J., Kaetzke, A., Kämpfer, P., Ludwig, W., and Fuchs, G. (1995) Taxonomic position of aromatic-degrading denitrifying Pseudomonad strains K 172 and KB 740 and their description as new members of the genera *Thauera*, as *Thauera aromatica* sp. nov., and *Azoarcus*, as *Azoarcus evansii* sp. nov., respectively, members of the beta subclass of the Proteobacteria. *Int J Syst Bacteriol* **45:** 327-333.

Barton, B.M., Harding, G.P., and Zuccarelli, J. (1995) A general method for detecting and sizing large plasmids. *Anal Biochem* **226:** 235-240.

Bellanger, X., Payot, S., Leblond-Bourget, N., and Guédon, G. (2014) Conjugative and mobilizable genomic islands in bacteria: evolution and diversity. *FEMS Microbiol Rev* **38:** 720-760.

Blázquez, B., Carmona, M., García, J.L., and Díaz, E. (2008) Identification and analysis of a glutaryl-CoA dehydrogenase-encoding gene and its cognate transcriptional regulator from *Azoarcus* sp. CIB. *Environ Microbiol* **10:** 474-482.

Boll, M., Löffler, C., Morris, B.E., and Kung, J.W. (2013) Anaerobic degradation of homocyclic aromatic compounds via arylcarboxyl-coenzyme A esters: organisms, strategies and key enzymes. *Environ Microbiol* **16:** 612-627.

Bozinovski, D., Taubert, M., Kleinsteuber, S., Richnow, H.H., von Bergen, M., Vogt, C., and Seifert, J. (2014) Metaproteogenomic analysis of a sulfate-reducing enrichment culture reveals genomic organization of key enzymes in

573 the *m*-xylene degradation pathway and metabolic activity of proteobacteria.
574 *Syst Appl Microbiol* **37:** 488-501.
575
576 Carmona, M., Zamarro, M.T., Blázquez, B., Durante-Rodríguez, G, Juárez, J.F.,
577 Valderrama, J.A., *et al*. (2009) Anaerobic catabolism of aromatic compounds: a
578 genetic and genomic view. *Microbiol Mol Biol Rev* **73:**71-133.
579
580 Choi, E.N., Cho, M.C., Kim, Y., Kim, C.K., and Lee, K. (2003) Expansion of
581 growth substrate range in *Pseudomonas putida* F1 by mutations in both *cymR*
582 and *todS*, which recruit a ring-fission hydrolase CmtE and induce the *tod*
583 catabolic operon, respectively. *Microbiology* **149:** 795-805.
584
585 de Lorenzo, V., and Timmis, K.N. (1994). Analysis and construction of stable
586 phenotypes in gram-negative bacteria with Tn*5*- and Tn*10*-derived
587 minitransposons. *Methods Enzymol* **235:** 386-405.
588 Don, R.H., and Pemberton, J.M. (1981) Properties of six pesticide degradation
589 plasmids isolated from *Alcaligenes paradoxus* and *Alcaligenes eutrophus*. *J*
590 *Bacteriol* **145:** 681-686.
591 Eaton, R.W., and Timmis, K.N. (1986) Characterization of a plasmid-specified
592 pathway for catabolism of isopropylbenzene in *Pseudomonas putida* RE204. *J*
593 *Bacteriol* **168:**123-131.
594 Fernández, H., Prandoni, N., Fernández-Pascual, M., Fajardo, S., Morcillo, C.,
595 Díaz, E., and Carmona, M. (2014) *Azoarcus* sp. CIB, an anaerobic biodegrader
596 of aromatic compounds shows an endophytic lifestyle. *PLoS One* **9:** e110771.
597 Fuchs, G., Boll, M., and Heider, J. (2011) Microbial degradation of aromatic
598 compounds - from one strategy to four. *Nat Rev Microbiol* **9:** 803-816..
599 Furukawa, K., Hirose, J., Suyama, A., Zaiki, T., and Hayashida, S. (1993) Gene
600 components responsible for discrete substrate specificity in the metabolism of
601 biphenyl (*bph* operon) and toluene (*tod* operon). *J Bacteriol* **175:** 5224-5232.
602 Gaillard, M., Pernet, N., Vogne, C., Hegenbüchle, O., and van der Meer,
603 J.R.(2008) Host and invader impact of the *clc* genomic island into
604 *Pseudomonas aeruginosa* PAO1. *Proc Nat Acad Sci USA* **105:**7058-7063.
605 Gaillard, M., Vallaeys, T., Jörg Vorhölter, F., Minoia, M., Werlen, C., Sentchilo,
606 V., *et al*. (2006) The *clc* element of *Pseudomonas* sp strain B13, a genomic
607 island with various catabolic properties. *J Bacteriol* **188:** 1999-2013.
608 Gao, F., and Zhang, C.T. (2006) GC-Profile: a web-based tool for visualizing
609 and analyzing the variation of GC content in genomic sequences. *Nucleic Acids*
610 *Res* **34:** W686-691.
611

612 Guglielmini, J., Néron, B., Abby, S.S., Garcillán-Barcia, M.P., de la Cruz, F.,
613 and Rocha, E.P. (2014) Key components of the eight classes of type IV secretion
614 systems involved in bacterial conjugation or protein secretion. *Nucleic Acids Res*
615 **42:** 5715-5727.

616 Guglielmini, J., Quintais, L., Garcillán-Barcia, M.P., de la Cruz, F., and Rocha,
617 E.P.C. (2011) The repertoire of ICE in prokaryotes underscores the unity,
618 diversity, and ubiquity of conjugation. PLoS Genetics 7: e1002222.
619

620 Hickey, W.J., Chen, S., and Zhao, J. (2012) *The phn* island: a new genomic
621 island encoding catabolism of polynuclear aromatic hydrocarbons. *Frontiers in*
622 *Microbiol* **3:**125.

623 Jin, H.M., Jeong, H., Moon, E.J., Math, R.K., Lee, K., Kim, H.J., *et al.* (2011)
624 Complete genome sequence of the polycyclic aromatic hydrocarbon-degrading
625 bacterium *Alteromonas* sp. strain SN2. *J Bacteriol* **193:** 4292-4293.

626 Juárez, J.F., Liu, H., Zamarro, M.T., McMahon, S., Liu, H., Naismith, J.H., *et al.*
627 (2015) Unraveling the specific regulation of the central pathway for anaerobic
628 degradation of 3-methylbenzoate. *J Biol Chem* **290:** 12165-12183.
629
630 Juárez, J.F., Zamarro, M.T., Eberlein, C., Boll, M., Carmona, M., and Díaz, E.
631 (2013) Characterization of the *mbd* cluster encoding the anaerobic 3-
632 methylbenzoyl-CoA central pathway. *Environ Microbiol* **15:** 148–166.
633
634 Juhas, M., van der Meer, J.R., Gaillard, M., Harding, R.M., Hood, D.W., and
635 Crook, D.W. (2009) Genomic island: tools of bacterial horizontal gene transfer
636 and evolution. *FEMS Microbiol Rev* **33:** 376-393.
637
638 Kim, S.J., Park, S.J., Jung, M.Y., Kim, J.G., Madsen, E.L., and Rhee, S.K.
639 (2014) An uncultivated nitrate-reducing member of the genus *Herminiimonas*
640 degrades toluene. *Appl Environ Microbiol* **80:** 3233-3243.
641
642 Lechner, M., Schmitt,K., Bauer,S., Hot, D., Hubans, C., Levillain, E., *et al.*
643 (2009) Genomic island excisions in *Bordetella petrii. BMC Microbiol* **9:**141
644

645 López-Barragán, M. J., Carmona, M., Zamarro, M. T., Thiele, B., Boll, M.,
646 Fuchs, G., *et al*. (2004) The *bzd* gene cluster, coding for anaerobic benzoate
647 catabolism, in *Azoarcus* sp. strain CIB. *J Bacteriol* **186:** 5762-5774.

648
649 Martín-Moldes, Z., Zamarro, M.T., del Cerro, C., Valencia, A., Gómez, M.J.,
650 Arcas, A, *et al.* (2015) Whole-genome analysis of *Azoarcus* sp. strain CIB
651 provides genetic insights to its different lifestyles and predicts novel metabolic
652 features. *Syst Appl Microbiol* **38:** 462-471.

Minoia, M., Gaillard, M., Reinhard, F., Stojanov, M., Sentchilo, V., and van der Meer, J.R. (2008) Stochasticity and bistability in horizontal transfer control of a genomic island in *Pseudomonas*. *Proc Natl Acad Sci USA* **105:** 20792-20797.

Miyazaki, R., and van der Meer, J.R. (2011) A dual functional origin of transfer in the ICE*clc* genomic island of *Pseudomonas knackmussi* B13. *Mol Microbiol* **79:** 743-758.

Miyazaki, R., Bertelli, C., Benaglio, P., Canton, J., de Coi, N., Gharib, W.H., *et al*. (2015) Comparative genome analysis of *Pseudomonas knackmussii* B13, the first bacterium known to degrade chloroaromatic compounds. *Environ Microbiol* **17:** 91-104.

Miyazaki, R., Minoia, M., Pradervand, N., Sulser, S., Reinhard, F., and van der Meer, J.R. (2012) Cellular variability of RpoS expression underlies subpopulation activation of an integrative and conjugative element. *PLoS Genet* **8:** e1002818.

Moreno-Ruiz, E., Hernáez, M.J., Martínez-Pérez, O., and Santero, E. (2003) Identification and functional characterization of *Sphingomonas macrogolitabida* strain TFA genes involved in the first two steps of the tetralin catabolic pathway. *J Bacteriol* **185:** 2026-2030.

Nishi, A., Tominaga, K., and Fukukawa, K. (2000) A 90-kilobase conjugative chromosomal element coding for biphenyl and salicylate catabolism in *Pseudomonas putida* KF715. *J Bacteriol* **182:** 1949-1955.

Nishizawa, T., Tago, K., Oshima, K., Hattori, M., Ishii, S., Otsuka, S., and Senoo, K. (2012) Complete genome sequence of the denitrifying and N_2O-reducing bacterium *Azoarcus* sp. strain KH32C. *J Bacteriol* **194:** 1255.

Ohtsubo, Y., Ishibashi, Y., Naganawa, H., Hirokawa, S., Atobe, S., Nagata, Y., and Tsuda, M. (2012) Conjugal transfer of polychlorinated biphenyl/biphenyl degradation genes in *Acidovorax* sp. strain KKS102, which are located on an integrative and conjugative element. *J Bacteriol* **194:** 4237-4248.

Pérez-Pantoja, D., de la Iglesia, R., Pieper, D.H., and González, B. (2008) Metabolic reconstruction of aromatic compounds degradation from the genome of the amazing pollutant-degrading bacterium *Cupriavidus necator* JMP134. *FEMS Microbiol Rev* **32:** 736-794.

Pflugmacher, U., Averhoff, B., and Gottschalk, G. (1996) Cloning, sequencing, and expression of isopropylbenzene degradation genes from *Pseudomonas* sp. strain JR1: identification of isopropylbenzene dioxygenase that mediates trichloroethene oxidation. *Appl Environ Microbiol* **62:** 3967-3977.

692 Pradervand, N., Delavat, F., Sulser, S., Miyazaki, R., and van der Meer J.R.
693 (2014a) The TetR-type MfsR protein of the integrative and conjugative element
694 (ICE) ICE*clc* controls both a putative efflux system and initiation of ICE
695 transfer. *J Bacteriol* **196:** 3971-3979.
696
697 Pradervand, N., Sulser, S., Delavat, F., Miyazaki, R., Lamas, I., and van der
698 Meer, J.R. (2014b) An operon of three transcriptional regulators controls
699 horizontal gene transfer of the integrative and conjugative element ICE*clc* in
700 *Pseudomonas knackmussii* B13. *PLoS Genet* **10:** e1004441.

701 Rabus, R., Boll, M., Heider, J., Meckenstock, R.U., Buckel, W., Einsle, O., *et al.*
702 (2016) Anaerobic microbial degradation of hydrocarbons: from enzymatic
703 reactions to the environment. *J Mol Microbiol Biotechnol* **26:** 5-28.

704 Rabus, R., Kube, M., Beck, A., Widdel, F., and Reinhardt, R. (2002) Genes
705 involved in the anaerobic degradation of ethylbenzene in a denitrifying
706 bacterium, strain EbN1. *Arch Microbiol* **178:** 506–516.

707 Rabus, R., Kube, M., Heider, J., Beck, A., Heitmann, K., Widdel, F., and
708 Reinhardt, R. (2005) The genome sequence of an anaerobic aromatic-degrading
709 denitrifying bacterium, strain EbN1. *Arch Microbiol* **183:** 27-36.

710 Ramos, J.L., Sol Cuenca, M., Molina-Santiago, C., Segura, A., Duque, E.,
711 Gómez-García, M.R., *et al.* (2015) Mechanisms of solvent resistance mediated
712 by interplay of cellular factors in *Pseudomonas putida*. *FEMS Microbiol Rev* **39:**
713 555-566.

714 Ravatn, R., Studer, S., Springael, D., Zehnder, A.J.B., and van der Meer, J.R.
715 (1998) Chromosomal integration, tandem amplification, and deamplification in
716 *Pseudomonas putida* F1 of a 105-kilobase genetic element containing the
717 chlorocatecol degradative genes from *Pseudomonas* sp. strain B13. *J Bacteriol*
718 **180:** 4360-4369.

719 Roche, D., Fléchard, M., Lallier, N., Répérant, M., Brée, A., Pascal, G., *et al.*
720 (2010) ICE*Ec*2, a new integrative and conjugative element belonging to the
721 pKLC102/PAGI-2 family, identified in *Escherichia coli* strain BEN374. *J*
722 *Bacteriol* **192:** 5026-5036.

723 Ryan, M.P., Pembroke, J.T., and Adley, C.C. (2009) Novel Tn*4371*-ICE like
724 element in *Ralstonia pickettii* and genome mining for comparative elements.
725 *BMC Microbiol* **9:** 242-259.

726 Sambrook, J., and Russell, D.W. (2001) *Molecular Cloning: A Laboratory*
727 *Manual*. Cold Spring Harbor, NY, USA: Cold Spring Harbor Laboratory Press.

728 Seah, S.Y., Terracina, G., Bolin, J.T., Riebel, P., Snieckus, V., and Eltis, L.D.
729 (1998) Purification and preliminary characterization of a serine hydrolase

involved in the microbial degradation of polychlorinated biphenyls. *J Biol Chem* **273:** 22943-22949.

Smillie, C., Garcillán-Barcia, M.P., Francia, M.V., Rocha, E.P.C., and de la Cruz, F. (2010) Mobility of plasmids. *Microbiol Mol Biol Rev* **74:** 434-452.

Springael, D., and Top, E.M. (2004) Horizontal gene transfer and microbial adaptation to xenobiotics: new types of mobile genetic elements and lessons for ecological studies. *Trends Microbiol* **12:** 53-58.

Toleman, M.A., and Walsh, T.R. (2011) Combinatorial events of insertion sequences and ICE in gram-negative bacteria. *FEMS Microbiol Rev* **35:** 912-935.

Toussaint, A., Merlin, M., Monchy, S., Benotmane, M.A., Leplae, R., Mergeay, M., and Springael, D. (2003) The biphenyl- and 4-chlorobiphenyl-catabolic transposon Tn*4371*, a member of a new family of genomic islands related to IncP and Ti plasmids. *Appl Environ Microbiol* **69:** 4837-4845.

Valderrama, J.A., Durante-Rodríguez, G., Blázquez, B., García, J.L., Carmona, M., and Díaz, E. (2012) Bacterial degradation of benzoate: cross-regulation between aerobic and anaerobic pathways. *J Biol Chem* **287:**10494-10508.

Van Houdt, R., Monchy, S., Leys, N., and Mergeay, M. (2009) New mobile genetic elements in *Cupriavidus metallireducens* CH34, their possible roles and occurrence in other bacteria. *Antonie van Leeuwenhoek* **96:** 205-226.

Wöhlbrand, L., Jacob, J.H., Kube, M., Mussmann, M., Jarling, R., Beck, A., *et al*. (2013) Complete genome, catabolic sub-proteomes and key-metabolites of *Desulfobacula toluolica* Tol2, a marine, aromatic compound-degrading, sulfate-reducing bacterium. *Environ Microbiol* **15:**1334-1355.

Wozniak, R.A.F., and Waldor, M.K. (2010) Integrative and conjugative elements: mosaic mobile genetic elements enabling dynamic lateral gene flow. *Nature Rev Microbiol* **8:** 552-563.

Yagi, J.M., Sims, D., Brettin, T., Bruce, D., and Madsen, E.L. (2009) The genome of *Polaromonas naphthalenivorans* strain CJ2, isolated from coal tar-contaminated sediment, reveals physiological and metabolic versatility and evolution through extensive horizontal gene transfer. *Environ Microbiol* **11:** 2253-2270.

Zylstra, G.J., and Gibson, D.T. (1989) Toluene degradation by *Pseudomonas putida* F1. Nucleotide sequence of the *todC1C2BADE* genes and their expression in *Escherichia coli*. *J Biol Chem* **264:**14940-14946.

Figure legends

Fig. 1. Scheme of the global structure of ICE$_{XTD}$ from *Azoarcus* sp. CIB and main aromatic hydrocarbon degradation pathways encoded.

A. Modular organization of the ICE$_{XTD}$ element. For ORF details see Supporting Information Table S1. The integration/excision, regulation, conjugation and partition modules are shown in red, blue, orange, and yellow bars. The three adaptation modules are shown in green bars. Regions containing genes encoding complete or truncated transposases are shown in white bars. The flanking *attL* and *attR* sites are also indicated. B. Proposed pathways for the degradation of aromatic hydrocarbons related to the adaptation modules 1 and 3 of ICE$_{XTD.}$ The aerobic (red arrows) and anaerobic (blue arrows) degradation pathways of toluene, cumene and *m*-xylene are shown. The peripheral and central pathways are indicated by discontinuous and continuous arrows, respectively. The enzyme names and predicted functions are detailed in Table S1. It should be noted that the central bzd pathway for anaerobic degradation of benzoyl-CoA (enzyme names in italics) is not encoded within the ICE$_{XTD}$ element but in a different chromosomal location (Martín-Moldes *et al.*, 2015). The names of the intermediate compounds are: 1, 3-methylcatechol; 2, 3-isopropylcatechol; 3, 2-hydroxy-6-oxo-6-methylhexa-2,4-dienoate; 4, 2-hydroxy-6-oxo-7-methylocta-2,4-dienoate; 5, 2-hydroxypenta-2,4-dienoate; 6, benzoyl-CoA; 7, 3-methylbenzoyl-CoA; 8, cyclohex-1,5-diene-1-carbonyl-CoA; 9, methyl-cyclohex-1,5-diene-1-carbonyl-CoA; 10, 3-hydroxypimelyl-CoA; 11, 3-hydroxy-6-methyl-pimelyl-CoA; 12, 3-hydroxy-4-methyl-pimelyl-CoA. So far it is still unknown whether the MbdY-catalyzed reaction produces compound 11 or 12. The black discontinuous arrows represent the lower pathways for the beta-oxidation of 3-hydroxypimelyl-CoA and 3-hydroxy-6-methyl-pimelyl-CoA or 3-hydroxy-4-methyl-pimelyl-CoA to central metabolites.

Fig. 2. Aromatic hydrocarbon-dependent expression of the ICE_{XTD} adaptation modules in *Azoarcus* sp. CIB. Agarose gel electrophoresis of RT-PCR products. Graphs below each gel represent the quantification of the band signal intensity (in arbitray units).

A. RT-PCRs of *Azoarcus* sp. CIB cells exponentially grown under oxic conditions with benzoate (lane B) or toluene (lane T) were performed as described in Materials and Methods, with the primer pairs (Supporting Information Table S2) that amplify the *todC1* gene (located in adaptation module 1).

B. RT-PCRs of *Azoarcus* sp. CIB cells exponentially grown under nitrate-reducing conditions with benzoate (lanes B), toluene (lanes T) or *m*-xylene (lanes X) were performed as described in Materials and Methods, with the primer pairs (Supporting Information Table S2) that amplify the *bssA*, *bbsD*, and *mbdO* genes (located in adaptation module 3).

C. RT-PCRs of anaerobically grown *Azoarcus* sp. CIB cells that were exposed (+) or not (-) to a sudden toluene shock. RT-PCRs were performed with the primer pairs that amplify the AzCIB_4437 and AzCIB_4432 genes located in adaptation module 2, as indicated in Materials and Methods.

Error bars in the graphs indicate the standard deviation of the values in three independent experiments.

Fig. 3. Tracking the location of ICE_{XTD} in *Azoarcus* sp. CIB cells.

A. Schematic representation of the integrated form of ICE_{XTD} and its excision from the *Azoarcus* sp. CIB chromosome. The *attL*, *attR*, *attP* and *attB* sites are indicated by grey symbols. The genes flanking the *att* sites are shown by solid gray arrows. The AzCIB_R0069 gene encoding the $tRNAGly^{CCC}$ integration site is shown by a black arrow. The location and orientation of P1-P4 primers used for the detection of the chromosome integrated (In), extrachromosomal circular (Ec), and repaired chromosome (Rc) forms of ICE_{XTD} are indicated by triangles.

B. PCR-based analysis of the ICE_{XTD} in *Azoarcus* sp. CIB cells. Total genomic DNA was obtained from *Azoarcus* sp. CIB cultures grown anaerobically with benzoate until exponential (CIB (Exp)) or stationary (CIB (Stat)) phase and was used as template to test the location of ICE_{XTD} by PCR. Total DNA obtained from *Azoarcus* sp. CIBT

cultures grown anaerobically with benzoate to reach stationary phase (CIBT) was also used as template to check for the presence of ICE_{XTD}. The primer pairs used to track the extrachromosomal circular form (Ec), the repaired chromosome (Rc), and the chromosome integrated form (In) of ICE_{XTD} were P3/P2, P1/P4 and P1/P2, respectively, and they are detailed in Supporting Information Table S2. Lanes M, molecular size markers (HaeIII-digested ϕX174 DNA). Numbers on the left represent the sizes of the markers (in bp).

C. Pulsed-field gel electrophoresis of *Azoarcus* sp. CIB and *Azoarcus* sp. CIBT cells grown anaerobically with benzoate. The preparation of cells and the conditions for the pulse-field gel electrophoresis are detailed in Materials and Methods. Gel was stained with GelRed (left panel) or subjected to southern blotting and hybridization with a ^{32}P-labeled bssA probe (right panel). The extrachromosomal form of ICE_{XTD} after linearization with S1 nuclease treatment is shown with an arrow. Lanes 1, *Azoarcus* sp. CIBT cells; lanes 2, *Azoarcus* sp. CIB cells; lanes 3, molecular size markers (lambda concatemers markers). Numbers represent the sizes of the markers (in kb).

Fig. 4. Growth of *Azoarcus* sp. CIBTRif and *Azoarcus* sp. CIBTRifICE_{XTD} strains alone or in competition experiments.

A. Compared growth curves between *Azoarcus* sp. CIBTRif (square symbols) and *Azoarcus* sp. CIBTRifICE_{XTD} (circle symbols) in minimal MC medium containing 3 mM benzoate as carbon source either aerobically (solid lines) or anaerobically (dashed lines).

B. Competition experiments between *Azoarcus* sp. CIBTRif and *Azoarcus* sp. CIBTRifICE_{XTD} inoculated in ratio of 50/50% in minimal MC medium with 3 mM benzoate as carbon source and grown anaerobically for 60 generations (ten subsequent transfers). Transfer 0 corresponds to the start of the experiment. Total population of *Azoarcus* sp. CIBTRif and *Azoarcus* sp. CIBTRifICE_{XTD} was determined as the total number of colonies per ml formed on MC-glutarate plates, set to 100%. The population of *Azoarcus* sp. CIBTRifICE_{XTD} was determined as colonies formed on MC-glutarate plates supplemented with kanamycin. The striped bars correspond to the relative population of *Azoarcus* sp. CIBTRifICE_{XTD} as percentage of the total bacterial

population. Values are the mean of three different experiments. Error bars indicate standard deviation.

Fig. 5. Growth effects of ICE_{XTD} in *C. pinatubonensis*.

A. Growth curves of *C. pinatubonensis* JMP289 (continuous line) and *C. pinatubonensis* JMP289ICE_{XTD} (discontinuous line) in minimal MC medium containing 0.2% succinate as sole carbon source under oxic conditions. Values are the mean of three different experiments. Error bars indicate standard deviation.

B. Growth curves of *C. pinatubonensis* JMP289 (continuous line) and *C. pinatubonensis* JMP289ICE_{XTD} (discontinuous line) in minimal MC medium containing *m*-xylene as sole carbon source under anoxic conditions (10 mM nitrate as terminal electron acceptor). Values are the mean of three different experiments. Error bars indicate standard deviation.

Fig. 6. Comparison of the general architecture of ICE_{XTD}-like elements from *Azoarcus* sp. CIB, "*A. aromaticum*" EbN1, and *A. toluclasticus* MF63 strains. The integration/excision, regulatory, conjugation and partition modules that constitute the core region of the ICEs are indicated in red, blue, orange and yellow colors. The adaptation modules are shown in green, and their encoded relevant functions are indicated. The *attL* and *attR* sites are also shown, and their locations at the CIB chromosome (Acc. No. CP011072), EbN1 chromosome (Acc. No. NC.006513), or at contig 2 of strain MF63 (Acc. No. NZ_KB899492), are indicated in kb. The $tRNAGly^{CCC}$ integration sites are shown by black arrows, and they correspond to AzCIB_R0069, Ebt19 and F464_RS0104335 locus tags in strains CIB, EbN1 and MF63, respectively. The flanking genes are indicated by grey arrows. The *sodC* gene corresponds to AzCIB_4574 and F464_RS27880 locus tags in strains CIB and MF63, respectively. The white bar in ICE^{EbN1} represents a region that contains a second copy of a truncated integrase (EbA2481 and EbA2486), a relaxase (EbA2492), and several paralogs of T4SS proteins (EbA2508-EbA2521).

Table 1. Bacterial strains used in this work.

Strain	Relevant genotype and main features[a]	Reference or source
Azoarcus strains		
Azoarcus sp. CIB	Wild type strain	López-Barragan *et al*., (2004)
Azoarcus sp. CIBd*tolR*	*Azoarcus* sp. CIB with an ICE_{XTD}-Km, Km^r	Laboratory strain collection
Azoarcus sp. CIBT	*Azoarcus* sp. CIB without ICE_{XTD}	This work
Azoarcus sp.CIBTRif	*Azoarcus* sp. CIBT, Rif^r	This work
Azoarcus sp.CIBTRifICE_{XTD}	*Azoarcus* sp. CIBTRif containing ICE_{XTD}-Km, Rif^r Km^r	This work
Azoarcus evansii	Wild-type strain	DSMZ 6898
*A. evansii*Rif	*A. evansii*, Rif^r	This work
*A. evansii*RifICE_{XTD}	*A. evansii*Rif containing ICE_{XTD}-Km, Km^r	This work
Cupriavidus strains		
Cupriavidus pinatubonensis JMP 289	*Cupriavidus pinatubonensis* JMP134, Rif^r	Don and Pemberton (1981)
C. pinatubonensis JMP289ICE_{XTD}	*C. pinatubonensis* JMP289 containing ICE_{XTD}-Km, Rif^r Km^r	This work

[a] The abbreviations used are as follows: Km^r, kanamicin-resistant; Rif^r, rifampicin-resistant

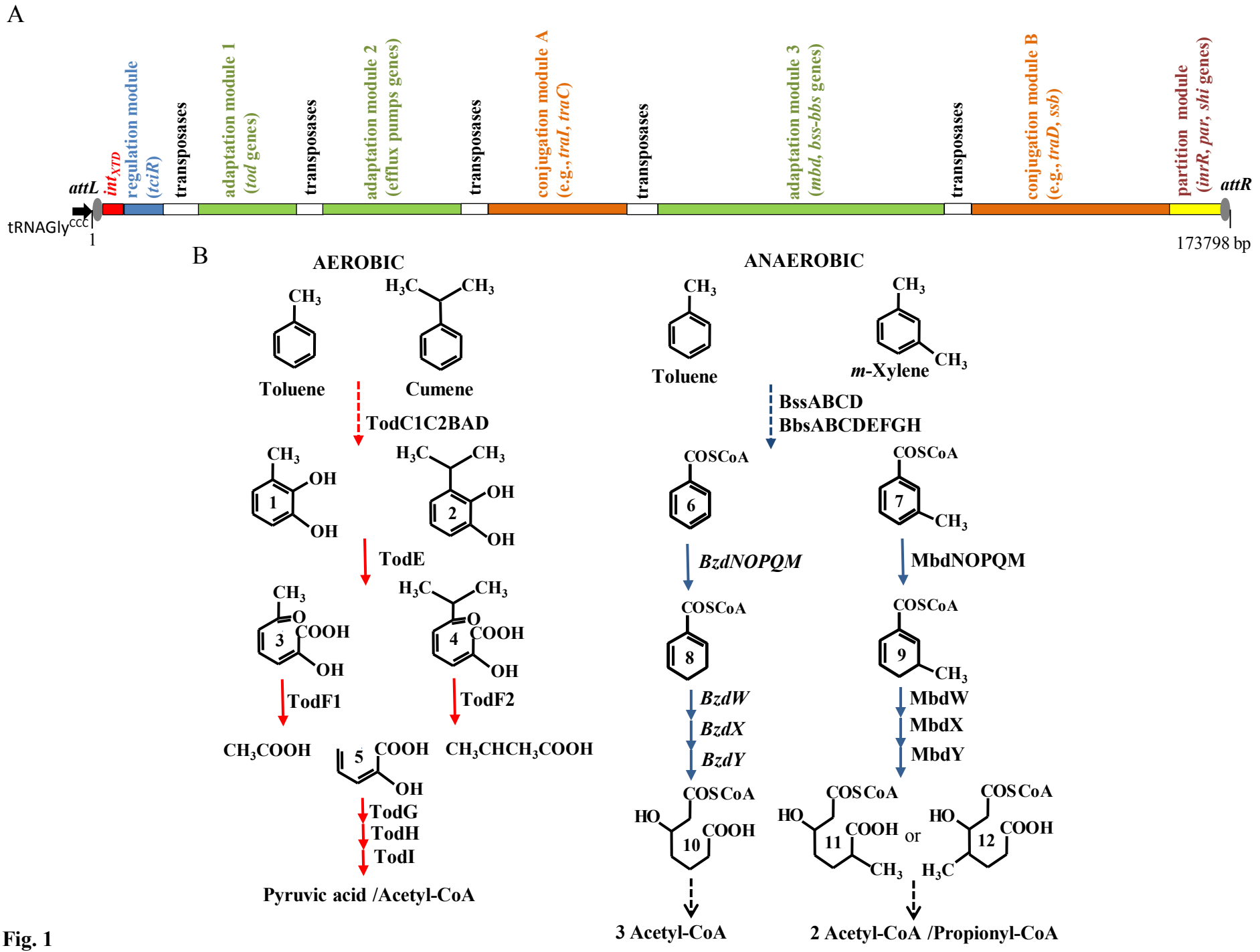
A
attL
int XTD
regulation module (tciR)
transposases
adaptation module 1 (tod genes)
transposases
adaptation module 2 (efflux pumps genes)
transposases
conjugation module A (e.g., traI, traC)
transposases
adaptation module 3 (mbd, bss-bbs genes)
transposases
conjugation module B (e.g., traD, ssb)
partition module (inrR, par, shi genes)
attR
tRNAGly CCC
1
173798 bp
B
AEROBIC
ANAEROBIC
Toluene
Cumene
m-Xylene
TodC1C2BAD
BssABCD
BbsABCDEFGH
COSCoA
TodE
BzdNOPQM
MbdNOPQM
TodF1
TodF2
BzdW
BzdX
BzdY
MbdW
MbdX
MbdY
CH3COOH
CH3CHCH3COOH
TodG
TodH
TodI
Pyruvic acid /Acetyl-CoA
3 Acetyl-CoA
2 Acetyl-CoA /Propionyl-CoA
or

Fig. 1

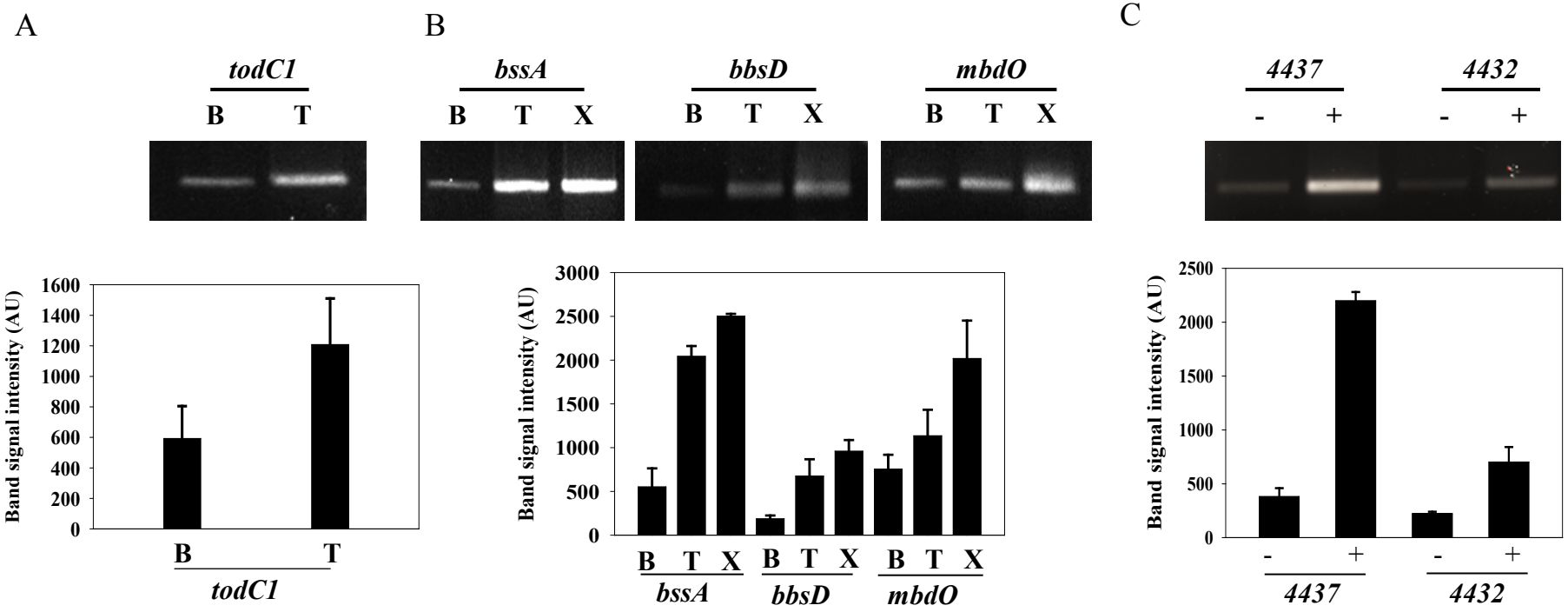
A
todC1
B
T
Band signal intensity (AU)
1600
1400
1200
1000
800
600
400
200
0
B
T
todC1
B
bssA
bbsD
mbdO
B T X
B T X
B T X
B T X
Band signal intensity (AU)
3000
2500
2000
1500
1000
500
0
B T X B T X B T X
bssA bbsD mbdO
C
4437
4432
- + - +
Band signal intensity (AU)
2500
2000
1500
1000
500
0
- + - +
4437 4432

Fig. 2

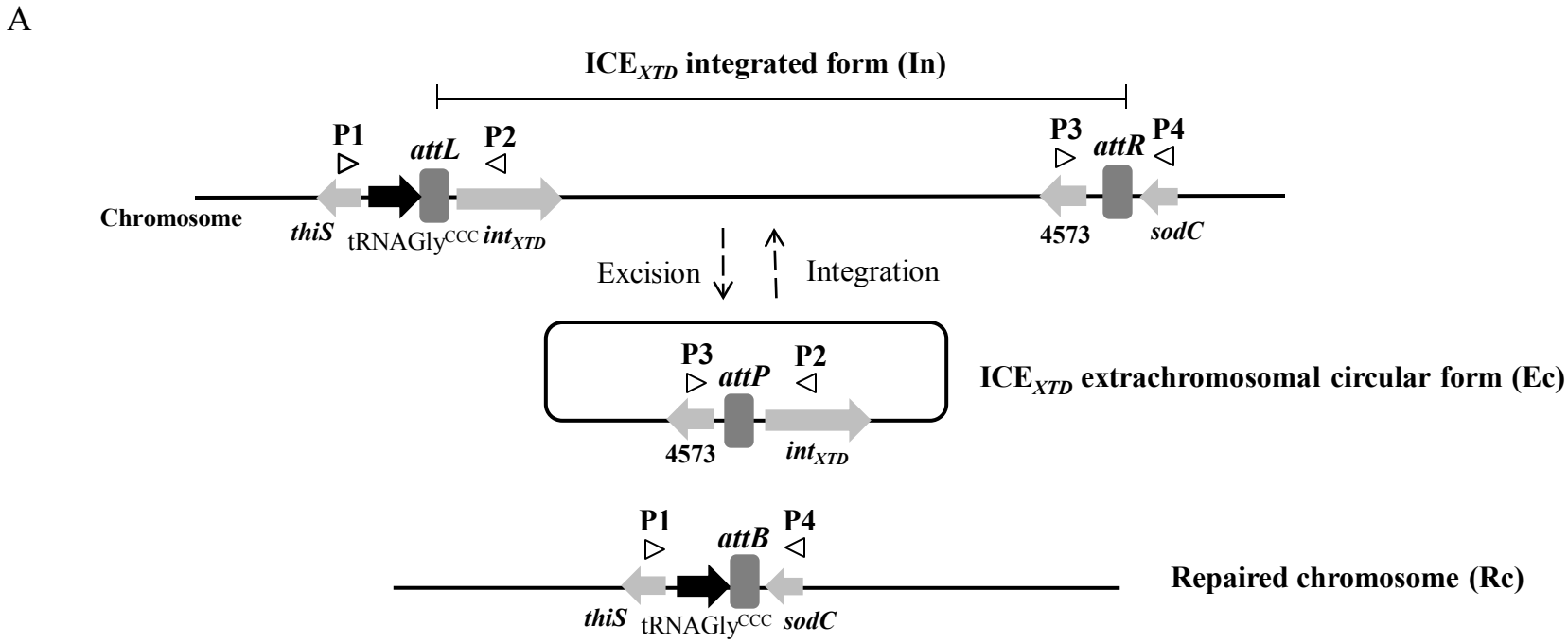
A
ICE$_{XTD}$ integrated form (In)
P1
attL
P2
P3
attR
P4
Chromosome
thiS
tRNAGly^{CCC}
int$_{XTD}$
4573
sodC
Excision
Integration
P3
attP
P2
4573
int$_{XTD}$
ICE$_{XTD}$ extrachromosomal circular form (Ec)
P1
attB
P4
thiS
tRNAGly^{CCC}
sodC
Repaired chromosome (Rc)

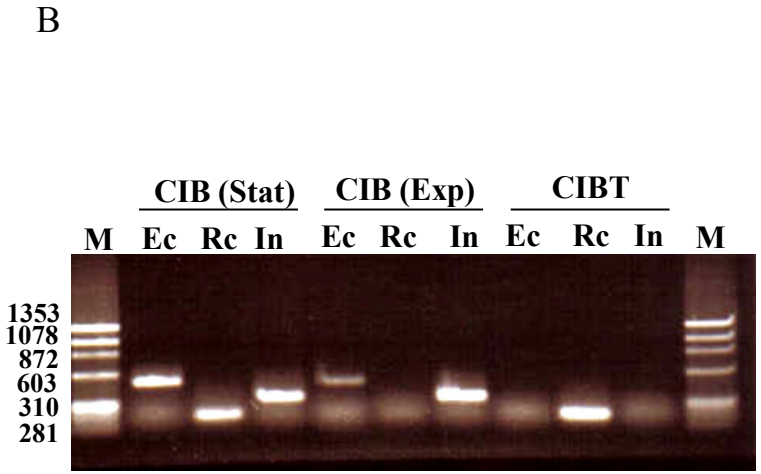
B
CIB (Stat)
CIB (Exp)
CIBT
M
Ec
Rc
In
Ec
Rc
In
Ec
Rc
In
M
1353
1078
872
603
310
281

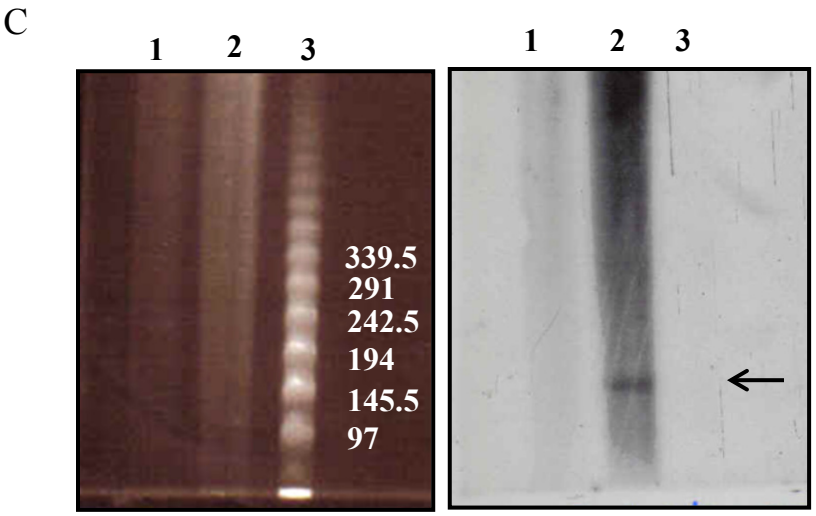
C
1
2
3
339.5
291
242.5
194
145.5
97
1
2
3

Fig.3

A

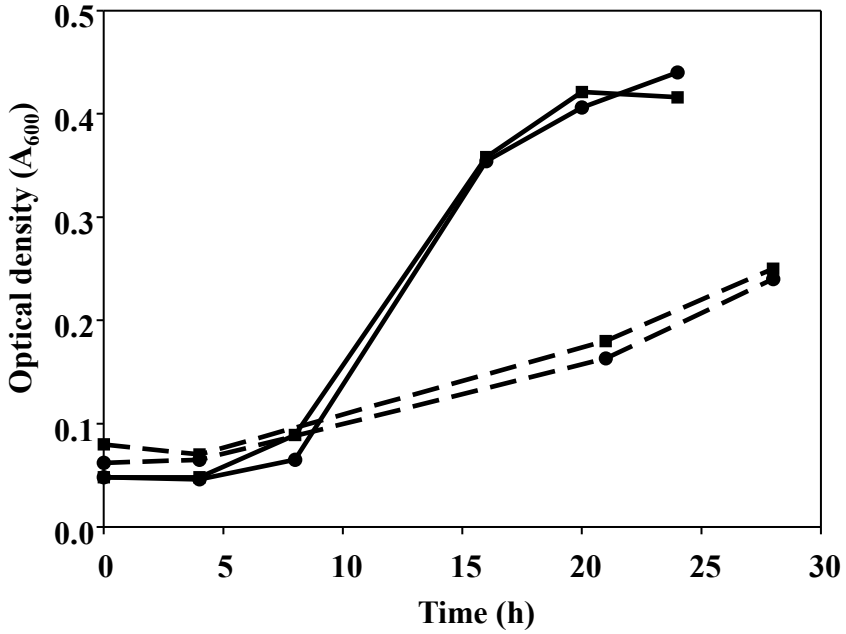
0.5
0.4
0.3
0.2
0.1
0.0
Optical density (A_{600})
0
5
10
15
20
25
30
Time (h)

B

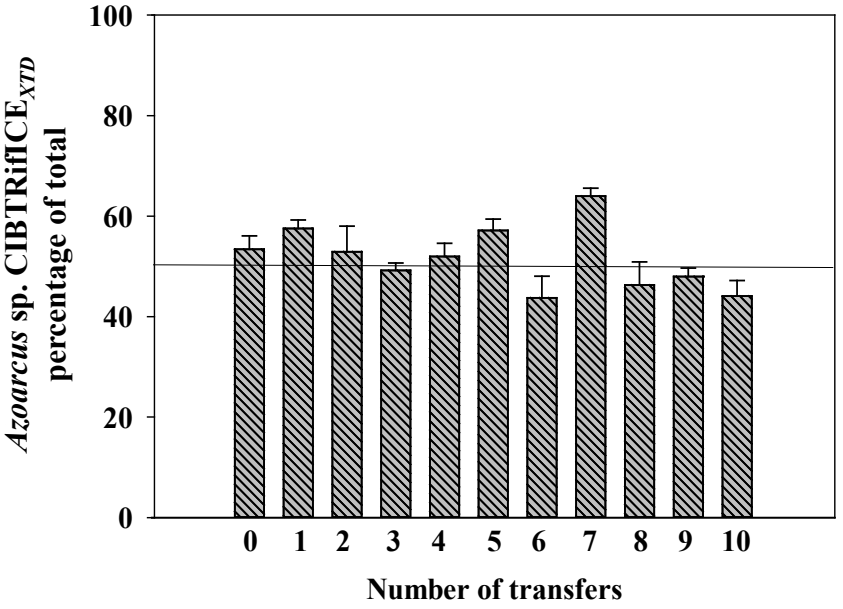
100
80
60
40
20
0
Azoarcus sp. CIBTRifICE$_{XTD}$
percentage of total
0
1
2
3
4
5
6
7
8
9
10
Number of transfers

Fig.4

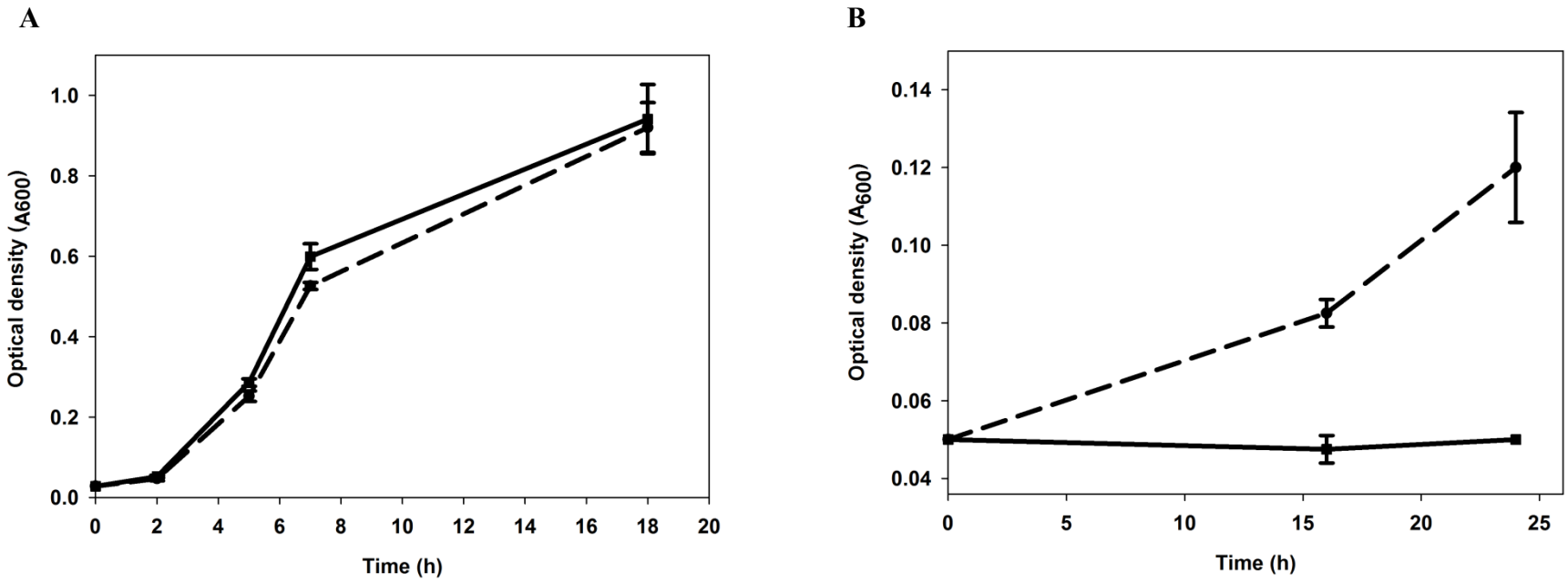
A
Optical density (A600)
1.0
0.8
0.6
0.4
0.2
0.0
0
2
4
6
8
10
12
14
16
18
20
Time (h)
B
Optical density (A600)
0.14
0.12
0.10
0.08
0.06
0.04
0
5
10
15
20
25
Time (h)

Fig.5

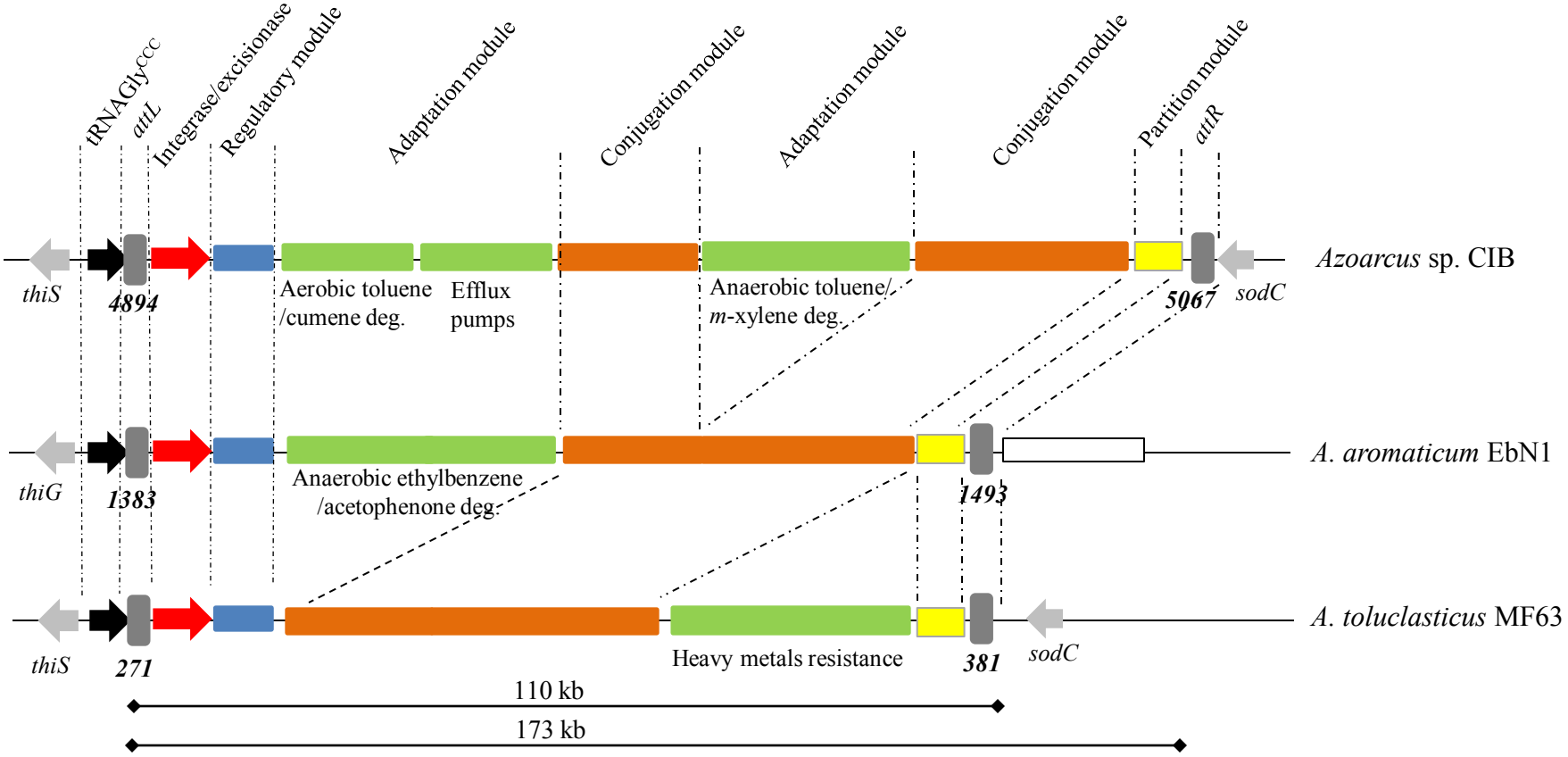
tRNAGly^CCC
attL
Integrase/excisionase
Regulatory module
Adaptation module
Conjugation module
Adaptation module
Conjugation module
Partition module
attR
thiS
4894
Aerobic toluene /cumene deg.
Efflux pumps
Anaerobic toluene/ m-xylene deg.
5067
sodC
Azoarcus sp. CIB
thiG
1383
Anaerobic ethylbenzene /acetophenone deg.
1493
A. aromaticum EbN1
thiS
271
Heavy metals resistance
381
sodC
A. toluclasticus MF63
110 kb
173 kb

Fig.6

Table 2. Growth phenotype of different bacterial strains in aromatic hydrocarbons.

Bacterial strain	Anaerobic growth on[a]		Aerobic growth on[a]	
	Toluene	*m*-Xylene	Toluene	Cumene
Azoarcus sp. CIB	+	+	+	+
Azoarcus sp. CIBT	–	–	–	–
Azoarcus sp.CIBTRifICE$_{XTD}$	+	+	+	+
A. evansii	–	–	–	–
*A. evansii*RifICE$_{XTD}$	+	+	+	+
C. pinatubonensis JMP289	–	–	+	–
C. pinatubonensis JMP289ICE$_{XTD}$	Nd	+	+	+

[a] Growth was tested in MC minimal medium containing the aromatic hydrocarbon as sole carbon source as indicated in Materials and Methods. +, growth; -, no growth. Nd, not determined.